Characteristics of ash and particle emissions during bubbling fluidised bed combustion of three types of residual forest biomass

João Peres Ribeiro[1*], Estela Domingos Vicente[1], Célia Alves[1], Xavier Querol[2], Fulvio Amato[2], Luís A. C. Tarelho[1]

[a] Centre for Environmental and Marine Studies, Department of Environment and Planning, University of Aveiro, 3810-193, Aveiro, Portugal

[b] Institute of Environmental Assessment and Water Research, IDAEA, Spanish Research Council (CSIC) 08034, Barcelona, Spain

Abstract

Combustion of residual forest biomass (RFB) derived from eucalypt (*Eucalyptus globulus*), pine (*Pinus pinaster*) and golden wattle (*Acacia longifolia*) was evaluated in a pilot-scale bubbling fluidised bed reactor (BFBR). During the combustion experiments, monitoring of temperature, pressure and exhaust gas composition has been made. Ash samples were collected at several locations along the furnace and flue gas treatment devices (cyclone and bag filter) after each combustion experiment, and were analysed for their unburnt carbon content and chemical composition. Total suspended particles (TSP) in the combustion flue gas were evaluated at the inlet and outlet of cyclone and baghouse filter, and further analysed for organic and elemental carbon, carbonates and 57 chemical elements. High particulate matter collection efficiencies, in the range 94-99%, were observed for the baghouse, while removal rates of only 1.4-17% were registered for the cyclone. .Due to the sand bed, Si was the major element in bottom ashes. Fly ashes, in particular those from eucalypt combustion, were especially rich in CaO, followed by relevant amounts of SiO_2, MgO and K_2O. Ash characteristics varied amongst experiments, showing that their inorganic composition strongly depends on both the biomass composition and combustion conditions. Inorganic constituents accounted for TSP mass fractions up to 40 wt.%

* Corresponding author. E-mail: joaoperes@ua.pt

Elemental carbon, organic matter and carbonates contributed to TSP mass fractions in the ranges 0.58% - 44%, 0.79% - 78% and 0.01% - 1.7%, respectively.

Keywords: Biomass combustion, Fluidised bed, Ash, Particulate matter

1. Introduction

The need for energy is a trademark of the world we live in and it has turned up the pressure on conventional fossil fuels, highlighting the environmental impacts of their conversion to useful energy. Thus, their subsistence as main primary energy resources in the short and medium term future is endangered. In this scenario, the need of alternative fuels that can partially replace fossil fuel in specific applications became clear. Biomass is among those alternatives, because it is considered renewable and neutral in terms of CO_2 emission. The carbon (CO_2) released during thermochemical conversion of biomass is considered equivalent to that captured by plants during photosynthesis, if a sustainable management of biomass resources is made (Faaji et al., 1998; Khan et al., 2009; Kumar and Singh, 2016).

Combustion has been the most widely used biomass thermochemical conversion process, and it has been applied for heating or for heat and power production (Basu, 2006; Van Loo and Koppejan, 2008). The main (gaseous) products of the process are carbon dioxide and water (Nunes et al. 2014). However, different types of fuels or incomplete combustion conditions may lead to noticeable production of other species of environmental relevance, such as CO, SO_2, NO_x, N_2O, among others (Amaral et al., 2014; Nunes et al., 2014; Okasha et al., 2014; Scala et al., 2013; Tarelho et al., 2011). Besides gaseous pollutant emissions, the combustion process also generates substantial particulate matter emissions. The increasing concern related to particulate matter emissions has been linked to the potential health and environmental hazardous effects associated mainly with their chemical constituents and size (Bølling et al., 2009; Luo et al., 2015). The particulate matter chemical and physical characteristics strongly depend on fuel characteristics, combustion technology and operating conditions (Amaral et al., 2014; Vicente et al., 2015; Wang and Fan, 2015).

The bubbling fluidised bed technology is one of the most widely used in industrial processes for heat and power production based on biomass fuels. This is a result of its many attractive characteristics, such as high combustion efficiency with a variety of fuels, either alone or combined (co-combustion regime), clean operation, high heat transfer rate between the solids bed and immersed surfaces, and simpler pre-processing of biomass fuels when compared to that required by competing combustion systems (Basu, 2006; Chirone et al., 2008; Nunes et al, 2015; Santos and Goldstein, 2008; Scala and Salatino, 2002).

Another main combustion product is ash. It can be defined as the inorganic part which is left after conversion of the organic fraction of the fuel, containing the bulk of the mineral fraction of the original biomass (Khan et al., 2009). The ash amount and characteristics after the combustion process reflect the composition of the biomass used as fuel, as well as the conversion technology and the operating conditions (Tarelho et al., 2015).

Ash-formation mechanisms are very complex, including a series of physical-chemical transformations encompassing segregation, evaporation, precipitation, nucleation and coalescence processes (Nunes et al., 2016). Factors influencing the composition of the ashes from biomass combustion include operating conditions, such as temperature, stoichiometry, air staging, additives, etc., and characteristics of the biomass, which in turn are dependent on factors such as plant species and age, growth process and conditions, fertilisers applied, harvesting time, among many others (Tarelho et al., 2012; Tarelho et al, 2015; Vassilev et al., 2010). Bottom ashes are usually coarser in size (Latva-Somppi et al., 1998a, b) and have higher density and lower specific surface area when compared to fly ashes (Tarelho et al., 2011).

Table 1 presents a compilation of bibliographical results for the determination of the relative abundances (%weight - wt - dry basis) of the major elements that constitute the inorganic fraction of (fly) ash obtained from biomass combustion by different techniques, such as fluidized bed or grate furnace combustion. The variability of results reflects the influence on ash composition of the type of biomass burnt but also of the technique chosen.

The aim of this work was to thoroughly characterize the ash characteristics and flue gas emissions for the combustion of residual biomass from forestry operations, including three typical Portuguese species, in a pilot-scale bubbling fluidised bed combustor. A novel aspect of this work was that the collection and analysis of ash and particle matter emissions have been made in

several points alongside the combustion system, rather than just in dedusting equipment. In this way, this work is more able to provide an integrated, more detailed, approach to the production of ash/particles in all relevant points of the entire combustion system, widening the existent knowledge in this field of research, and applying it to the Portuguese reality.

2. Materials and Methods

Distinct types of residual forest biomass were used as fuel during combustion experiments performed in a pilot-scale bubbling fluidised bed reactor (BFBR). The reactor is made of AISI 310 SS and has a combustion chamber with circular section (internal diameter of 0.25 m) and about 2.3 m height. The bed, with about 20 kg weight, was composed of sand (around 98.3 %wt. SiO_2), sieved in the range between 355 and 710 μm, and had a static height of about 0.23 m of bed, 0.14 of them above the primary (fluidising) air injectors.

The air supply was staged into primary and secondary air. Primary (fluidising) air was fed through injectors located in a distributor plate at the base of the reactor, with secondary air being fed from a tube located in the freeboard at 0.43 m above the distributor plate. Primary air accounted for 80% of total combustion air, corresponding to a flow of 12 $Nm^3 \cdot h^{-1}$, and a fluidising velocity between 2.5 and 3 times the minimum fluidising velocity, depending on the bed temperature. Secondary air flow rate was adjusted to represent 20% of the total combustion air supply (3 $Nm^3 \cdot h^{-1}$). This way, the hydrodynamic characteristics of the BFBR were maintained similar throughout the experiments. The stoichiometry of operation was controlled by adjusting the fuel feeding rate; the biomass feeding was performed at the bed surface by a system equipped with a screw feeder (Figure 1).

The reactor was equipped with a set of nine water-cooled probes located at different points along the reactor height, two of them inside the bed and six on the freeboard, plus one at the reactor exhaustion. Each probe was assembled with a K-type thermocouple plus a cerablanket filter at its tip. These probes allow the continuous monitoring of temperature and pressure along the reactor.

The combustion flue gas was sampled from the exhaust by means of a 180 ºC heated line and carried to a Fourier transform infrared gas analyser (FTIR Gasmet, CX 4000), which enabled the real-time and continuous monitoring of the gas composition for, amongst other, H_2O, CO_2 and

120 CO. Additionally, the O_2 composition was monitored on the dry gas by means of a paramagnetic
121 analyser (ADC model O2-700 with a Servomex Module). O_2 concentration (dry gas) in the flue
122 gases during the experiments was in the ranges 4.2-5.8, 3.4-4.8 and 4.9-5.8 for the combustion
123 of RFB derived from eucalypt, pine, and golden wattle, respectively.
124 Residual forest biomass (RFB) from eucalypt (*Eucalyptus globulus*), pine (*Pinus pinaster*) and
125 golden wattle (*Acacia longifolia*) was used as fuel in the combustion experiments. This biomass
126 consisted of tree tops and small braches resulting from forestry operations as logging activities
127 for the pulp and paper industry and other wood related industries, and also from forest
128 maintenance for wildfire prevention. The RFB was chipped and air dried, followed by sieving. In
129 order to achieve suitable particle size for the biomass feeding system, eucalypt and golden wattle
130 residues were sieved to dimensions below 5 mm, or less than 10 mm in the case of pine. The
131 chemical composition of the solid biomass used as fuel is shown in Table 2. All chemical analyses
132 were made according to international CEN/TS standards.
133 Ash samples were collected after each combustion experiment at several points along the pilot-
134 scale installation, namely: i) at the bottom bed (bottom ash - BA), ii) in the reactor's freeboard
135 inner wall at three points at different heights, from now on referred to as bottom, middle and top
136 (BFBR-B, BFBR-M and BFBR-T, respectively), iii) in the reactor exit flue gas duct, at two points
137 at increasing distance from the reactor exit and from now on designated as flue gas duct first
138 section (FA-1) and second section (FA-2), iv) at the cyclone (FA_Cy), and v) at the baghouse
139 filter (FA_BagH). Immediately after collection, ash samples were stored in closed bags to prevent
140 any moisture absorption. The samples were then processed according to standard CEN/TS
141 14775:2004 for unburnt organic matter content determination, and digested according to the
142 international standard CEN/TS 15290:2006, with the suitable ratio of the four recommended
143 reagents: 2 mL of 30% (w/w) hydrogen peroxide (H_2O_2), 3 mL of 65% (w/w) nitric acid (HNO_3)
144 and 0.75 mL of 40% (w/w) hydrofluoric acid (HF), plus 7.5 mL of 4% (w/w) boric acid (H_3BO_3),
145 and 20 mL distilled water, all of them commercial, analytical grade, reagents. The digestion
146 procedure was performed in a Berghof Speedwave® Four microwave system, with TFM™
147 digestion vessels. The cooled digested solutions were then transferred to 100 mL volumetric
148 flasks. Major elements, namely sodium (Na), potassium (K), calcium (Ca), magnesium (Mg),
149 silicon (Si), iron (Fe), manganese (Mn), aluminium (Al), as well as some minor elements, namely

zinc (Zn) and copper (Cu), were analysed in a PerkinElmer AAnalyst 200 Atomic Absorption Spectrometer.

Total suspended particles (TSP) were sampled under isokinetic conditions when the fluidised bed combustor was operated under steady-state conditions. A low volume sampler unit (TCR, TECORA, model 2.004.01) operating at a gas flow rate of 0.6 $m^3 \cdot h^{-1}$ (at atmospheric pressure and temperature) was used to collect TSP onto quartz filters directly from the combustion flue gas at the inlet and outlet of the cyclone and baghouse filter ducts. Although the Portuguese legislation on emissions (Ordinance nº 675/2009 of 23th June). requires monitoring of TSP, a multistage cascade impactor, designed according to standard ISO 23210:2009 for the nozzle dimensioning, that allows separation into 3 particulate size fractions (below 2.5 μm, between 2.5 and 10 μm, and above 10 μm) was applied in 3 replicate experiments to the exhaust duct downstream the baghouse filter in order to assess the emissions for each different particulate size fraction. The quartz filters were pre-baked at 500ºC for 6 hours to remove any organic contaminants. The mass deposited in the filters was determined by gravimetry using a microbalance (RADWAG 5/2Y/F). The organic (OC) and elemental carbon (EC) of the particulate matter samples were analysed using a thermal-optical transmission technique, thoroughly described elsewhere (Gonçalves et al., 2014), after a previous sample acidification to remove carbonates. These latter were determined by sample acidification with phosphoric acid (Calvo et al., 2013). The analysis of major and trace elements was performed by Inductively Coupled Plasma Atomic Emission Spectrometry (ICP-AES) and Inductively Coupled Plasma Mass Spectrometry (ICP-MS) techniques, as proposed by Querol et al. (2001). The detection limits were 0.01 ng m^{-3} for most of the trace elements analysed.

3. Results and Discussion

The temperatures along the BFBR, for the nine measurement points previously explained, are represented in Figure 2. Similar temperature profiles along the combustion system operating with chipped biomass from eucalypt and pine could be observed. For the chipped golden wattle experiment, greater temperature variations between probes at different heights could be verified. At the sand bed level, the temperature value was the lowest of the eight measurements made along the BFBR (about 800 ºC), regardless of the chipped biomass fuel used. Immediately above

180 that level, as shown by the results of thermocouple T3, temperatures can be about 40 to 50 ºC
181 higher. The exception was the chipped pine combustion experiments, in which similar
182 temperature at those height levels were observed. Maximum temperature levels were registered
183 in the middle of the BFBR (thermocouples T4 to T7), with values of up to 1030 ºC for the
184 combustion of eucalypt and pine, and up to 1100 ºC for the combustion of golden wattle. These
185 highest temperatures registered in the freeboard above the secondary air and biomass feeding
186 location have been reported in the literature (Tarelho et al., 2011) and can be explained by the
187 release and combustion of the volatile matter present in the fuel (typically quite high in biomass).
188 Most of this volatile matter is released during the heating stage of the fuel particles as they enter
189 the high temperature region of the BFBR, burning around and above this location, as stated in
190 previous studies (Tarelho et al., 2015).
191 In the upper zone of the freeboard (monitored by thermocouple T8), temperatures were slightly
192 lower for the experiments with eucalypt and pine, given the increasing distance to where biomass
193 is fed (and burnt). The experiment with golden wattle showed once again a different trend, with
194 temperatures at the T8 point being about 100 ºC higher than the ones registered for the other two
195 tested fuels. As may be seen by the results of thermocouple T9, the exhaust gas leaves the BFBR
196 and enters the dedusting equipment at a temperature that varied in the range of 450 to 530 ºC,
197 depending on the experiment.
198 The composition of the exit flue gas in terms of its main constituents (CO_2 and CO) is shown in
199 Figure 3 for all three combustion experiments. Despite feeding with chipped pine was easier than
200 eucalypt, because of the greater homogeneity of the fuel, the CO_2/CO concentrations in the exit
201 flue gas were quite similar. The first oscillated roughly between 13 and 17%, while the higher
202 peaks of CO were always lower than 2,000 ppm. Golden wattle proved to be the hardest fuel to
203 feed to the BFBR, because of its heterogeneity, low density and high content in fibrous material.
204 This caused higher fluctuation in the CO_2 content (between 11 to 18%), as well as high contents
205 of CO in the flue gas, with peaks of up to 20 000 ppm.
206 Figure 4 shows the unburnt organic matter content of the ashes collected after the combustion
207 experiments of eucalypt, pine and golden wattle (%weight, db). Regardless of the fuel, ashes
208 collected from either the bed sand, the interior of the BFBR or the cyclone separator (especially
209 efficient in removing coarser particles) showed practically no unburnt organic matter (<4% dry

basis). Ashes collected from the middle of the BFBR inside wall after the eucalypt combustion experiment showed, however, slightly higher organic matter contents (almost 7% dry basis). In the exhaust duct, ashes collected after combustion of pine or golden wattle had about 8-9% (db) organic matter. The baghouse filter retained particles that are much richer in organic matter. For example, for the golden wattle experiment, about 90% of those particles' mass was organic matter. For the eucalypt combustion experiment, ashes with higher organic matter content (about 25%, db) were collected in the exhaust duct, before the dust separators. Regarding this result, it is worth recalling that the temperature at this location for eucalypt combustion was about 35-40 ºC lower than for the combustion of pine or golden wattle.

The chemical composition of bottom and fly ashes collected along the combustion system, for the three combustion experiments, is shown in Figure 5. A significantly different composition between bottom ash and fly ash can be seen. Bottom ash mainly comprises Si (>90% db), since it is almost entirely composed by the original silica sand used as bed. Minor amounts (<2%) of CaO, K_2O, Na_2O or Fe_2O_3 have also been found in bottom ash. Ashes collected at the bottom "layer" of the BFBR wall show very similar composition to bottom ashes, with Si being the most abundant constituent, followed by CaO and Fe_2O_3, in the case of BFBR_B ashes from the combustion of chipped pine. In the middle and top layers inside the BFBR, sampled ashes showed a composition more similar to the one of fly ashes, with high amounts of CaO (up to 50% in the combustion of pine and golden wattle and up to 80% in the combustion of eucalypt), but also MgO, K_2O and even Fe_2O_3 (up to 15-20% in some cases). Higher amounts of Si in the pine and golden wattle combustion experiments (between 20-30%) were also registered, since Si accounts for 5 to 15% of the content of these biomass types. For the eucalypt biomass sample, no Si was detected, justifying the lower content in Si in its ashes (all sampling points above BFBR_B level).

With respect to fly ashes, figures show that the composition of the ashes collected at the exhaust duct (FA_1 and FA_2), and at the cyclone separator (FA_Cy), are especially rich in CaO, reflecting the original composition of the biomass. For the combustion of eucalypt, the CaO content in these ashes reached values of up to 75-90% (since 70% of the original biomass inorganic fraction was CaO), with some considerable amounts of MgO and K_2O (6-12%) as well. These values are somewhat higher than the ones reported in the literature (see Table 1), because of the lack of Si in the composition of the original biomass and, consequently, in the ashes. Ashes

collected after the combustion of pine and golden wattle also showed predominance of CaO in their chemical composition, but with lower contents (35 to 45% for fly ash from the exhaust, and 50-60% for fly ash from the cyclone separator). SiO_2 was the other dominant component, thus confirming the trend found in the literature. Once again, MgO and K_2O showed some relevant contribution to the inorganic fraction of those ashes, with contents in the range of 5-8% (both oxide species) for pine combustion and in the range of 10-15% MgO and 6-17% K_2O for golden wattle combustion. K_2O and CaO were the most abundant compounds in baghouse-filter ashes for eucalypt and pine combustion. In the case of golden wattle, little CaO was found in that class of fly ash, whereas the content of Fe_2O_3 was strangely higher than any result found in the literature. Fly ash from the baghouse-filter (FA_BagH) also showed some abundance of Na_2O in its composition (4-10%). MnO_2 never made up more than 3% of the chemical composition of any ash from any combustion experiment, which falls within the literature range. The only biomass type that showed potential to produce aluminum rich ashes was pine, with Al_2O_3 content reaching 6% for cyclone ashes. This reflects the presence of aluminum in pine's chemical composition, with an abundance of about 3%, which is not true for the eucalypt or golden wattle used in the experiments. In what minor elements are concerned, neither Zn nor Cu showed worrying concentrations in the ashes from combustion of biomass (always lower than 0.25%).

The reported chemical composition of the biomass ashes makes this material suitable for a variety of applications, especially two: i) incorporation in cement-based materials, depending on ash characteristics (such as unburnt carbon and inorganic composition), which can alter concrete properties like workability, setting and mechanical strength (Berra et al., 2015; Cuenca et al., 2013; Niu et al, 2016; Ohenoja et al. 2016a; Ohenoja et al., 2016b; Rajamma et al, 2015); and ii) incorporation in soil as fertiliser, given that biomass ash pH is typically in the range 8-13 and its richness in soil nutrients like Ca, K or Mg (Demeyer et al., 2001; Niu et al 2016; Nkana et al., 1998; Odlare and Pell, 2009; Park et al., 2005; Perucci et al., 2008; Saarsalmi et al., 2012).

As already stated, the scope of this work was not exclusively centered on bottom and fly ashes deposited at different points along the combustion facility, but also on finer particles that have the capacity to leave the facility with the flue gas. Once those fine and ultrafine particles surpass the gas cleaning equipment and reach the environment, they have the ability to penetrate deep in the

269 respiratory tract when inhaled and for that reason have been reported to cause stronger harmful
270 effects on public health than coarse particles (Avino and Manigrasso, 2016; Luo et al., 2015). In
271 this work, the size segregation tests allowed us to conclude that a mass fraction higher than 90%
272 of the total particulate matter emitted was concentrated in the fraction below 2.5 μm, before the
273 dust separators.
274 Concerning the Portuguese regulation, the TSP emission values were normalised to volumetric
275 oxygen content (O_2 ref.) of 11%v in the exhaust gas. Figure 6 shows the TSP emissions from the
276 combustion experiments of eucalypt, pine and golden wattle (mg Nm^{-3}, 11%v O_2). It should be
277 noted that the emission limit stipulated by the Portuguese Ordinance nº 675/2009 is 150 mg TSP
278 Nm^3. The lowest TSP emissions were registered for the combustion experiment of coniferous
279 biomass, which can be likely related to the more stable feeding of chipped pine. The cyclone
280 separator showed low efficiency in particle removal (5.1-13%) due to the small size of the particles
281 released. The baghouse filter system is known for providing high separation efficiencies for flue
282 gas cleaning. In the present study, collection efficiencies ranging from 94 to 98% were registered.
283 The detailed chemical composition of TSP emissions is presented in Tables 3, 4 and 5 for
284 eucalypt, pine and golden wattle combustion, respectively. The OC mass was converted to total
285 mass of organic matter (OM) using an OM/OC ratio of 1.55 (Calvo et al., 2013) in order to account
286 for oxygen, hydrogen, and some other atoms present in the organic material. Regardless of the
287 fuel burnt, the OM/TSP ratio was always lower downstream the baghouse filter. Only a few
288 percent (1 to 5 wt.%) of the TSP mass consisted of organic matter before and after the cyclone,
289 which is in agreement with published data (Calvo et al., 2013; Vicente et al., 2015). The OM
290 fractions in particulate matter from pine and golden wattle combustion before the dust separator
291 were 7 to 9 times lower than those obtained after the baghouse. For eucalypt, the difference was
292 much higher. The carbonate content in TSP samples was lower (always below 2%wt.) than the
293 values reported in the literature (Calvo et al., 2013; Vicente et al., 2015). The TSP inorganic
294 fraction showed different abundances, depending on the fuels and sampling points, with values
295 ranging from 24.1 to 41.8 wt.% before the cyclone, 29.8 to 42.7 wt.% after the cyclone and from
296 5.78 to 19.9 wt.% after the baghouse filter. It should be noted that the mass fraction is
297 underestimated not only due to fact that other elements, such as Si, were not analysed, but also

298 because most of the elements are present in the form of oxides. The mass fraction here reported
299 is not accounting for the unmeasured oxygen.
300 Moreover, a part of the unaccounted mass is likely to consist of water associated with particles
301 (Tsyro, 2005). Regardless of the fuel burnt, the composition of the samples collected at the
302 exhaust duct and after the cyclone was similar. Samples collected during eucalypt combustion
303 showed high amounts of K (24%) and Ca (13 %wt.) before and after the cyclone. S, Mg and Na
304 were present in minor amounts (0-2 %wt.). As regards the samples from golden wattle
305 combustion, the dominant element was once again K (14-20 %wt.) and other relevant constituents
306 were Na (3-4%), Ca (1-3%) and S (1-2 %wt.). In samples from pine combustion, the dominant
307 components before and after the cyclone were Ca (10-16 %wt.), K (9-11 %wt.), Mg (3 %wt.) and
308 S (2-3%wt.). Potassium is mainly found in submicron particles (Nussbaumer, 2003). Its content
309 in samples from pine combustion was lower than in samples from other biofuels, which is in
310 agreement with previous studies (Schauer et al., 2001). The Al content in particles from pine
311 combustion showed a slight decrease from the inlet to the outlet cyclone duct, which explains the
312 high content of this oxide in the ashes of this dedusting equipment.
313 Most elements were removed by the baghouse with a collection efficiency ranging from 17%
314 (golden wattle combustion) to 83% (eucalypt combustion). A relative enrichment of some volatile
315 elements, such as Zn, Mo, Ba and Ni, was observed in samples collected after the baghouse filter
316 from eucalypt and pine combustion. These findings are in accordance with previous studies
317 (Gogebakan and Selçuk, 2009; Hao et al., 2008). Golden wattle samples presented a relative
318 enrichment in Zn. The condensation of these elements onto particles during the flue gas travel
319 through the baghouse leads to a less efficient capture of the more volatile elements by dust
320 separators (Hao et al., 2008).
321

322 **4. Conclusions**

323 Bottom ashes mainly consisted of Si (>90 %wt. when expressed as SiO_2, dry basis), regardless
324 of the biomass type, since they are almost entirely constituted by the original silica sand used as
325 bed. Fly ashes were especially rich in CaO (particularly after eucalypt combustion) with some
326 relevant amounts of SiO_2, MgO and K_2O as well. Ashes collected inside the combustion chamber
327 tended to become more alike to the fly ash with increasing height. Ashes strongly reflect the

328 composition of the fuel that gave origin to them in the first place. Also, combustion conditions
329 (temperature, available oxygen for oxidation, etc.) may play an important role in the process of
330 ash formation, alongside the chemical behaviour of the biomass particles, in ways that are very
331 hard to comprehend or predict. The fuel composition and characteristics greatly affect TSP
332 emissions. The particulate emissions from golden wattle combustion were 2 times higher than
333 those observed for pine combustion, indicating that the physical characteristics, such as the
334 breakability of the fuel particles, can affect the transport by the screw feeder which, in turn,
335 influences the combustion behaviour. At the exhaust duct, the TSP emissions were mainly
336 composed of inorganic matter, while organic compounds represented a higher fraction at the
337 baghouse filter outlet duct. The dominant inorganic species in TSP samples showed fluctuations
338 depending on the fuel. The main elements in particles were K, Ca and Na. High collection
339 efficiencies were recorded for the baghouse filter. This cleaning device decreased significantly
340 emissions of either particles or their elemental constituents. Significant compositional differences
341 of exhaust gases and ashes from distinct combustion experiments were observed. . It became
342 clear that the specific physical-chemical characteristics of each one of the three biofuels, together
343 with varying operating conditions in the BFBR, are the main factors affecting ash and particulate
344 matter emissions and characteristics.
345 The emission factors derived from this study are potentially useful for improving emission
346 inventories of industrial combustion processes involving similar biofuels. Moreover, the TSP
347 detailed chemical databases can be eventually used as source input data in receptor modelling
348 (e.g. Chemical Mass Balance) to apportion the contribution of these combustion processes to the
349 atmospheric aerosol.
350

351 **Acknowledgments**

352 The authors acknowledge the Portuguese Foundation for Science and Technology for the
353 financial support through the project PTDC/AAC-AMB/116568/2010 (Project nº. FCOMP-01-
354 0124-FEDER-019346) - BiomAshTech-Ash impacts during thermo-chemical conversion of
355 biomass. Chemical analyses of particulate matter were funded by the European Commission
356 through the project “AIRUSE – Testing and development of air quality mitigation measures in
357 Southern Europe”, LIFE 11 ENV/ES/000584.

References

Amaral S, Junior J, Costa M, Neto T, Dellani R, Leite L (2014) Comparative study for hardwood and softwood forest biomass: Chemical characterization, combustion phases and gas and particulate matter emissions. Bioresource Technology. 164:55-63

Avino P, Manigrasso M (2016) Dynamic of submicrometer particles in urban environment. Environ Sci Pollut Res. DOI: 10.1007/s11356-016-6752-8

Basu P (2006) Combustion and gasification in fluidized beds, First ed. CRC Press Francis Group, Boca Raton, London and New York.

Berra M, Mangialardi T, Paolini A (2015) Reuse of woody biomass fly ash in cement-based materials. Constr. Build. Mater. 76:286–296.

Calvo A, Tarelho L, Teixeira E, Alves C, Nunes T, Duarte M, Coz E, Custódio D, Castro A, Artiñano B, Fraile R (2013) Particulate emissions from the co-combustion of forest biomass and sewage sludge in a bubbling fluidised bed reactor. Fuel Process. Technol. 114:58–68.

Chirone R, Salatino P, Scala F, Solimene R, Urciuolo M (2008) Fluidized bed combustion of pelletized biomass and waste-derived fuels. Combust. Flame 155:21–36.

Cuenca J, Rodríguez J, Martín-Morales M, Sánchez-Roldán Z, Zamorano M (2013) Effects of olive residue biomass fly ash as filler in self-compacting concrete. Constr. Build. Mater. 40:702–709.

Demeyer A, Nkana J, Verloo M (2001) Characteristics of wood ash and influence on soil properties and nutrient uptake : an overview. Bioresour. Technol. 77:287-295.

Esteves T, Rajamma R, Soares D, Silva A, Ferreira V, Labrincha J (2012) Use of biomass fly ash for mitigation of alkali-silica reaction of cement mortars. Constr. Build. Mater. 26:687–693.

Faaij A, Meuleman B, Turkenburg W, Van Wijk A, Bauen A, Rosillo-Calle A, Hall D (1998) Externalities of biomass based electricity production compared with power generation from coal in the Netherlands. Biomass and Bioenergy 14:125–147.

384 Girón R, Ruiz B, Fuente E, Gil R, Suárez-Ruiz I (2013) Properties of fly ash from forest biomass
385 combustion. Fuel 114:71-77.

386 Gogebakan Z, Selçuk N (2009) Trace elements partitioning during co-firing biomass with lignite
387 in a pilot-scale fluidized bed combustor. J. Hazard. Mater. 162:1129–1134.

388 Gonçalves C, Alves C, Nunes T, Rocha S, Cardoso J, Cerqueira M, Pio C, Almeida S, Hillamo
389 R, Teinilä K (2014) Organic characterization of PM10 in Cape Verde under Saharan dust
390 influxes. Atmos. Environ. 89:425–432.

391 H. Yi, J. Hao, L. Duan, X. Tang, P. Ning, X. Li (2008) Fine particle and trace element emissions
392 from an anthracite coal-fired power plant equipped with a bag-house in China. Fuel 87:2050–
393 2057 (in Chinese).

394 Ingerslev M, Skov S, Sevel L, Pedersen L (2011) Element budgets of forest biomass
395 combustion and ash fertilisation – A Danish case-study. Biomass and Bioenergy 35:2697–2704.

396 Kalembkiewicz J, Chmielarz U (2012) Ashes from co-combustion of coal and biomass: New
397 industrial wastes. Resour. Conserv. Recycl. 69:109–121.

398 Khan A, de Jong W, Jansens PJ, Spliethoff H (2009) Biomass combustion in fluidized bed
399 boilers: Potential problems and remedies. Fuel Process. Technol. 90:21–50.

400 Kocbach Bølling A, Pagels J, Yttri K, Barregard L, Sallsten G, Schwarze P, Boman C (2009)
401 Health effects of residential wood smoke particles: the importance of combustion conditions and
402 physicochemical particle properties. Part. Fibre Toxicol. 6:29.

403 Kumar R, Singh R (2016) An investigation in 20 kWth oxygen-enriched bubbling fluidized bed
404 combustor using coal and biomass. Fuel Processing Technology. 148:256-268

405 Latva-Somppi J, Kauppinen E, Valmari T, Ahonen P, Gurav S, Kodas T, Johanson B (1998)
406 The ash formation during co-combustion of wood and sludge in industrial fluidized bed boilers.
407 Fuel Process. Technol. 54:79–94.

408 Latva-Somppi J, Moisio M, Kauppinen E, Valmari T, Ahonen P, Tapper U, Keskinen J (1998)
409 Ash formation during fluidized-bed incineration of paper mill waste sludge. J. Aerosol Sci.
410 29:461–480.

411 Li L, Yu C, Bai J, Wang Q, Luo Z (2012) Heavy metal characterization of circulating fluidized
412 bed derived biomass ash. J. Hazard. Mater. 233–234:41–47.

413 Luo C, Zhu X, Yao C, Hou L, Zhang J, Cao J, Wang A (2015) Short-term exposure to particulate
414 air pollution and risk of myocardial infarction: a systematic review and meta-analysis. Environ
415 Sci Pollut Res 22:14651–14662.

416 Niu Y, Tan H, Hui S (2016) Ash-related issues during biomass combustion: Alkali-induced
417 slagging, silicate melt-induced slagging (ash fusion), agglomeration, corrosion, ash utilization,
418 and related countermeasures. Progress in Energy and Combustion Science. 52:1-61

419 Nkana J, Demeyer A, Verloo M (1998) Chemical Effects Of Wood Ash on Plant Growth in
420 Tropical Acid Soils. Bioresour. Technol. 63:251–260.

421 Nunes L, Matias J, Catalão J (2014) Mixed biomass pellets for thermal energy production: A
422 review of combustion models. Applied Energy. 127:135-140

423 Nunes L, Matias J, Catalão J (2016) Biomass combustion systems: A review on the physical
424 and chemical properties of the ashes. Renew. Sustain. Energy Rev. 53:235–242.

425 Nussbaumer T (2003) Combustion and Co-combustion of Biomass: Fundamentals,
426 Technologies, and Primary Measures for Emission Reduction. Energy and Fuels 17:1510–1521.

427 Odlare M, Pell M (2009) Effect of wood fly ash and compost on nitrification and denitrification in
428 agricultural soil. Appl. Energy 86:74–80.

429 Ohenoja K, Tanskanen P, Peltosaari O, Wigren V, Österbacka J, Illikainen M (2016a) Effect of
430 particle size distribution on the self-hardening property of biomass-peat fly ash from a bubbling
431 fluidized bed combustion. Fuel Processing Technology. 148:60-66

432

433 Ohenoja K, Tanskanen P, Wigren V, Kinnunen P, Körkkö M, Peltosaari O, Österbacka J,
434 Illikainen M (2016b) Self-hardening of fly ashes from a bubbling fluidized bed combustion of
435 peat, forest industry residuals, and wastes. Fuel. 165:440-446

436 Okasha F, Zaater G, El-Emam S, Awad M, Zeidan E (2014) Co-combustion of biomass and
437 gaseous fuel in a novel configuration of fluidized bed: Combustion characteristics. Fuel
438 133:143–152.

439 Park B, Yanai R, Sahm J, Lee D, Abrahamson L (2005) Wood ash effects on plant and soil in a
440 willow bioenergy plantation. Biomass and Bioenergy 28:355–365.

441 Perucci P, Monaci E, Onofri A, Vischetti C, Casucci C (2008) Changes in physico-chemical and
442 biochemical parameters of soil following addition of wood ash: A field experiment. Eur. J. Agron.
443 28:155–161.

444 Querol X, Alastuey A, Rodriguez S, Plana F, Ruiz C, Cots N, Massagué G, Puig O (2001) PM_{10}
445 and $PM_{2.5}$ source apportionment in the Barcelona Metropolitan area, Catalonia, Spain. Atmos.
446 Environ. 35:6407–6419.

447 Rajamma R, Senff L, Ribeiro M, Labrincha J, Ball R, Allen G, Ferreira V (2015) Biomass fly ash
448 effect on fresh and hardened state properties of cement based materials. Compos. Part B Eng.
449 77:1–9.

450 Saarsalmi A, Smolander A, Kukkola M, Moilanen M, Saramäki J (2012) 30-Year effects of wood
451 ash and nitrogen fertilization on soil chemical properties, soil microbial processes and stand
452 growth in a Scots pine stand. For. Ecol. Manage. 278:63–70.

453 Santos F, Goldstein L (2008) Experimental aspects of biomass fuels in a bubbling fluidized bed
454 combustor. Chem. Eng. Process. Process Intensif. 47:1541–1549.

455 Scala F, Salatino P (2002) Modelling fluidized bed combustion of high-volatile solid fuels. Chem.
456 Eng. Sci. 57:1175–1196.

457 Scala F, Solimene R, Montagnaro F (2013) Conversion of solid fuels and sorbents in fluidized
458 bed combustion and gasification. In: Scala F (Ed.) Fluidized bed technologies for near-zero
459 emission combustion and gasification. Woodhead Publishing Limited, Oxford, pp. 319–387.

460 Schauer J, Kleeman M, Cass G, Simoneit B (2001) Measurement of Emissions from Air
461 Pollution Sources. C1 to C29 Organic Compounds from Fireplace Combustion of Wood.
462 Environ. Sci. Technol. 35:1716–1728.

463 Tarelho L, Coelho A, Teixeira E, Rajamma E, Ferreira V (2011) Characteristics of ashes from
464 two Portuguese biomass co-generation plants. 19th European Biomass Conference &
465 Exhibition.

466 Tarelho L, Lopes M, Silva D, Freire M, Teixeira E, Modolo R (2014) Characteristics of biomass
467 used as fuel and ashes produced in two thermal power plants with BFBC. World Bioenergy
468 2014 - Conference & Exhibition on Biomass for Energy vol. 7.

469 Tarelho L, Neves D, Matos A (2011) Forest biomass waste combustion in a pilot-scale bubbling
470 fluidised bed combustor. Biomass and Bioenergy 35:1511–1523.

471 Tarelho L, Ribeiro J, Teixeira E, Vicente E, Matos A (2015) Forest biomass combustion in a
472 pilot-scale bubbling fluidized bed: influence of fuel properties and characteristics of ashes
473 produced. European Biomass Conference & Exhibition.

474 Tarelho L, Teixeira E, Silva D, Modolo R, Labrincha J, Rocha F (2015). Characteristics of
475 distinct ash flows in a biomass thermal power plant with bubbling fluidised bed combustor.
476 Energy. 90:387-402

477 Tarelho L, Teixeira E, Silva D, Modolo R, Silva J (2012) Characteristics, management and
478 application of ashes from thermochemical conversion of biomass to energy. World Bioenergy
479 2012 - Conference & Exhibition on Biomass for Energy.

480 Tsyro SG (2005) To what extent can aerosol water explain the discrepancy between model
481 calculated and gravimetric PM_{10} and $PM_{2.5}$? Atmos. Chem. Phys. 5:515–532.

482 Vamvuka D, Kakaras E (2011) Ash properties and environmental impact of various biomass
483 and coal fuels and their blends. Fuel Process. Technol. 92:570–581.

484 Vamvuka D, Zografos D, Alevizos G (2008) Control methods for mitigating biomass ash-related
485 problems in fluidized beds. Bioresour. Technol. 99:3534–3544.

Van Loo S, Koppejan J (2008) The Handbook of Biomass Combustion & Co-Firing, First ed. Earthscan, London.

Vassilev S, Baxter D, Andersen L, Vassileva C (2010) An overview of the chemical composition of biomass. Fuel 89:913–933.

Vassilev S, Baxter D, Andersen L, Vassileva C (2013) An overview of the composition and application of biomass ash. Part 1. Phase-mineral and chemical composition and classification. Fuel 105:40–76.

Vicente E, Tarelho L, Teixeira E, Duarte M, Nunes T, Colombi C, Gianelle V, Rocha G, de la Campa A, Alves C (2015) Emissions From the Combustion of Eucalyptus and Pine Chips in a Fluidised Bed Reactor (In Press). J. Environ. Sci. http://dx.doi.org/10.1016/j.jes.2015.07.012

Wang D, Fan L (2013) Particle characterization and behavior relevant to fluidized bed combustion and gasification systems. In: Scala F (Ed.) Fluidized bed technologies for near-zero emission combustion and gasification. Woodhead Publishing Limited, Oxford, pp. 42–73.

499 Table 1. Typical chemical composition of fly ash from combustion of biomass, from several
500 studies

	wt. % (dry basis)									Reference
	SiO_2	Al_2O_3	Fe_2O_3	CaO	K_2O	MgO	Na_2O	MnO	TiO_2	
Wood Pellets	4.3	1.3	1.5	55.9	16.8	8.5	0.6	7.62	0.10	(Khan et al., 2009)
Pine	32.5-45.8	4.5-4.6	2.9-3.5	25.7-49.2	2.5-8.2	0.4-3.6	0.4-0.6	ND	0.3-0.4	(Ingerslev et al., 2011; Nunes et al., 2016; Tarelho et al., 2014; Vamvuka and Kakaras, 2011)
Eucalypt	7.0-50.0	2.0-11.3	2.0-5.18	25.0-40.0	2.07-5.0	2.00-6.63	0.8-3.3	0.4-0.7	0.2-0.3	(Girón et al., 2013; Esteves et al., 2012; Rajamma et al., 2015; Tarelho et al., 2012)
Mix of woody and forest residues	17.0-50.5	3.12-15.1	2.32-5.18	14.0-44.4	2.78-16.0	1.65-9.34	0.46-2.85	0.20-1.32	0.2-0.96	(Demeyer et al., 2001; Li et al., 2012; Odlare and Pell 2009; Ohenoja et al., 2016b; Rajamma et al., 2015; Tarelho et al., 2012, 2014, 2015; Vassilev et al., 2013)
Herbaceous and Agricultural biomass	33.4-70.0	0.40-3.66	0.40-3.26	5.00-14.9	15-26.65	1.5-5.62	0.5-2.29	0.21	0-0.18	(Vamvuka and Kakaras, 2011; Vassilev et al., 2013)
Wheat straw	43.9-78.0	0.40-3.60	0.50-2.00	3.70-17.7	7.00-30.0	1.80-4.66	0.20-14.50	0.09	0.16	(Khan et al., 2009; Nunes et al., 2016; Vamvuka and Kakaras, 2011; Vassilev et al., 2013)
Sunflower pellets	2.9	0.6	0.8	21.6	22.8	21.6	0.24	0.129	0.10	(Khan et al., 2009)
Olive cake pellets	12.8	2.9	3.0	17.5	47.9	4.9	3.9	0.129	0.2	(Khan et al., 2009)
Olive kernel	30.0-67.7	7.0-20.3	0.05-14.0	10.0-22.9	9.2-13.0	3.0-4.0	0.9-11.2	<1.0	<1.0	(Nunes et al., 2016; Vamvuka and Kakaras, 2011; Vamvuka et al., 2008)
Olive husk	32.7	8.4	6.3	14.5	4.3	4.2	26.2	<1.0	<1.0	(Nunes et al., 2016)
20% Pellets+80% coal	77.29	12.26	2.97	1.66	0.92	6.12	0.61	ND	0.70	(Kalembkiewicz and Chmielarz, 2012)
50% wood chips+50%coal	28.50	15.11	7.70	14.19	2.23	5.00	1.46	ND	0.48	(Kalembkiewicz and Chmielarz, 2012)
20% forest residues+80% coal	ND	23.40	16.00	26.60	ND	5.30	2.97	0.11	0.50	(Kalembkiewicz and Chmielarz, 2012)

501 ND – Non detectable

502 Table 2. Chemical composition of the residual forest biomass used as fuel

Fuel	Proximate Analysis (%wt)				Elemental Analysis (%wt, db[a])				
	Moisture Content (as received)	Ash Content (db[a])	Volatile Matter Content (db[a])	Fixed Carbon (db[a])	C	H	O [c]	N	S
Eucalypt	10.98	2.87	81.50	15.63	43.99	7.94	47.12	0.03	nd[b]
Pine	12.67	1.23	79.84	18.93	48.48	6.30	43.76	0.15	ndl[b]
Golden Wattle	11.99	1.62	79.31	19.07	46.91	6.15	44.43	0.89	nd[b]

503 [a] dry basis; [b] not detected, below detection limit (100 ppm); [c] computed by difference

504 Table 3. TSP chemical composition from eucalypt combustion in weight percentage (wt.%).

Eucalypt	Before cyclone	After cyclone	After baghouse filter
EC	0.710	1.76	0.583
OM	0.789	1.59	77.7
Carbonates	0.008	0.011	0.005
Al	0.094	bdl	bdl
Ca	13.4	13.4	1.10
Fe	0.064	0.027	0.481
K	23.7	24.3	0.757
S	1.33	1.74	1.05
Mg	1.05	1.08	0.411
Na	1.06	1.11	bdl
P	0.271	0.250	0.618
Li	0.001	0.001	bdl
V	0.005	0.003	0.142
Cr	0.370	0.335	0.090
Mn	0.079	0.080	0.018
Cu	0.013	0.014	0.006
Zn	0.019	0.018	0.355
As	0.001	0.001	0.009
Rb	0.160	0.158	0.043
Sr	0.109	0.107	0.058
Mo	0.014	0.012	0.397
Ba	0.042	0.040	0.095
Pb	0.013	0.011	0.002
Ni	0.005	0.004	0.141
Ge	bdl	bdl	0.005
Cs	0.002	0.001	bdl
W	0.002	0.002	bdl

505 Note: Be, Ti, Co, Zr, Nb, Sn, Sb, La, Ce, Pr, Nd, Sm, Eu, Bi, Th, Ga, Y, Gd, Dy, Ho, Er, Tm, Lu, Hf, Ta, U, B, Sc, Tb, Yb,
506 Se, Cd and Tl were all below the detection limit (bdl).

507 Table 4. TSP chemical composition from pine combustion in weight percentage (wt.%).

	Before cyclone	After cyclone	After baghouse filter
EC	28.7	34.0	43.9
OM	4.90	3.52	43.1
Carbonates	0.889	0.706	0.146
Al	1.01	0.564	bdl
Ca	9.81	15.8	bdl
Fe	0.41	0.25	0.036
K	8.78	10.6	3.75
S	1.77	2.76	2.14
Mg	2.75	3.28	0.525
Na	0.419	0.734	bdl
P	0.529	0.620	0.417
V	0.004	0.008	bdl
Cr	0.587	0.745	bdl
Mn	0.226	0.294	bdl
Cu	0.010	0.012	0.058
Zn	0.070	0.096	0.229
As	0.001	0.002	bdl
Rb	0.045	0.056	bdl
Sr	0.036	0.053	0.041
Zr	bdl	bdl	0.244
Mo	0.030	0.034	0.279
Ba	0.029	0.034	0.153
Pb	0.007	0.008	bdl
Ni	0.027	0.023	0.182
Cs	0.001	bdl	bdl
W	0.002	0.004	bdl

508 Note: Li, Be, Ti, Co, Nb, Sn, Sb, La, Ce, Pr, Nd, Sm, Eu, Bi, Th, Ga, Ge, Y, Gd, Dy, Ho, Er, Tm, Lu, Hf, Ta, U, B, Sc, Tb,
509 Yb, Se, Cd and Tl were all below the detection limit (bdl).

510 Table 5. TSP chemical composition from golden wattle combustion in weight percentage (wt.%).

	Before cyclone	After cyclone	After baghouse filter
EC	23.2	16.2	12.5
OM	1.41	3.19	9.87
Carbonates	0.762	0.804	1.74
Al	0.071	bdl	bdl
Ca	1.27	2.50	0.20
Fe	0.052	0.069	0.039
K	17.1	20.3	13.7
S	1.12	1.56	1.20
Mg	0.393	0.762	0.097
Na	3.41	3.97	3.91
P	0.069	0.116	bdl
Li	0.003	0.003	0.002
V	0.001	bdl	bdl
Cr	0.355	0.264	0.185
Mn	0.030	0.036	0.014
Cu	0.019	0.017	bdl
Zn	0.030	0.023	0.242
As	0.001	bdl	bdl
Rb	0.084	0.069	0.027
Sr	0.008	0.011	0.001
Zr	0.001	bdl	0.003
Mo	0.024	0.016	bdl
Ba	0.007	0.008	0.004
Pb	0.005	0.005	0.001
Ni	0.002	0.002	0.001
Cs	0.001	0.001	bdl
W	0.005	0.003	0.003
B	bdl	bdl	0.223

511 Note: Be, Ti, Co, Nb, Sn, Sb, La, Ce, Pr, Nd, Sm, Eu, Bi, Th, Ga, Ge, Y, Gd, Dy, Ho, Er, Tm, Lu, Hf, Ta, U, Sc, Tb, Yb,

512 Se, Cd and Tl were all below the detection limit (bdl).

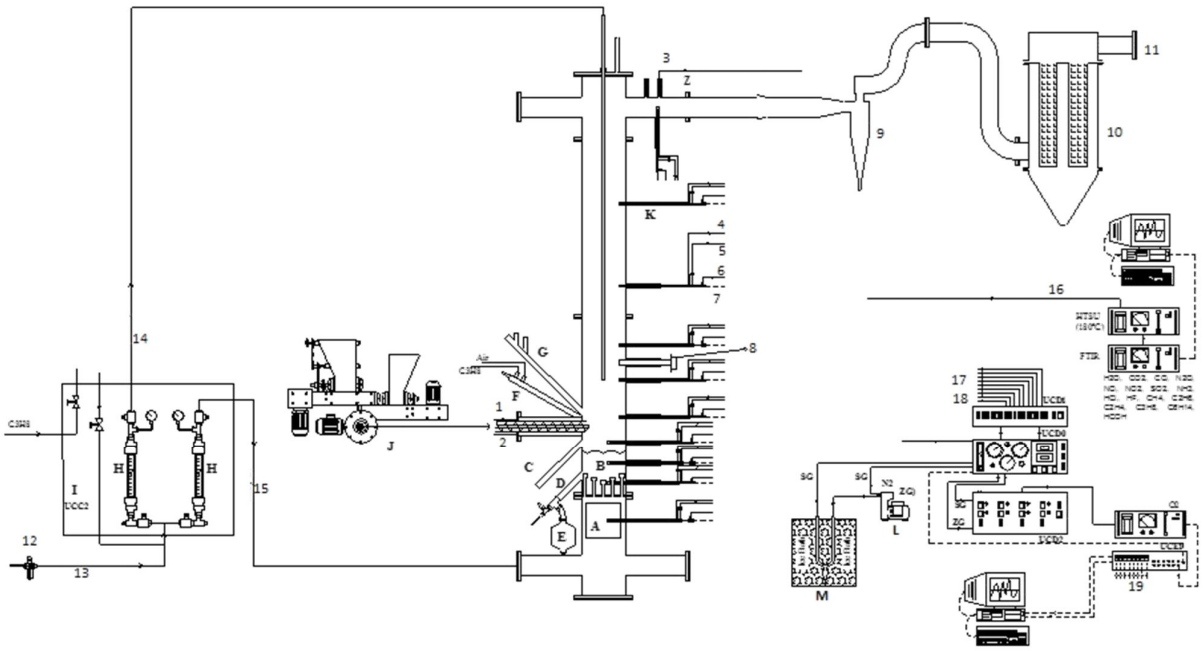

513

514 Figure 1. Schematic representation of the experimental facility with the pilot-scale BFB combustor. Dashed line —
515 Electric circuit, Solid line — Pneumatic circuit, A - Primary air heating system, B - Sand bed, C - Bed solids level control,
516 D - Bed solids discharge, E - Bed solids discharge silo, F - Propane burner system, G - Port for visualisation of bed
517 surface, H - Air flow meter (primary and secondary air), I - Control and command unit, J - Biomass feeder, K - Water-
518 cooled gas sampling probe, L - Gas sampling pump, M - Gas condensation unit for moisture removal, Z – Flue gas duct;
519 1,4 – Cold water (in), 2,5 – Warm water (out), 3, 16 – Heated sampling line (180 °C, 6, 18 – Pressure, 7,19 –
520 Temperature, 8 – Zirconia cell probe for O2 (ZC), 9 – Cyclone, 10 – House-bag filter, 11 – Exit flue gases to fan, 12 –
521 Pressure regulators, 13 – Compressed dry air, 14 – Secondary air, 15 – Primary air, 17 – Sample gas (SG)

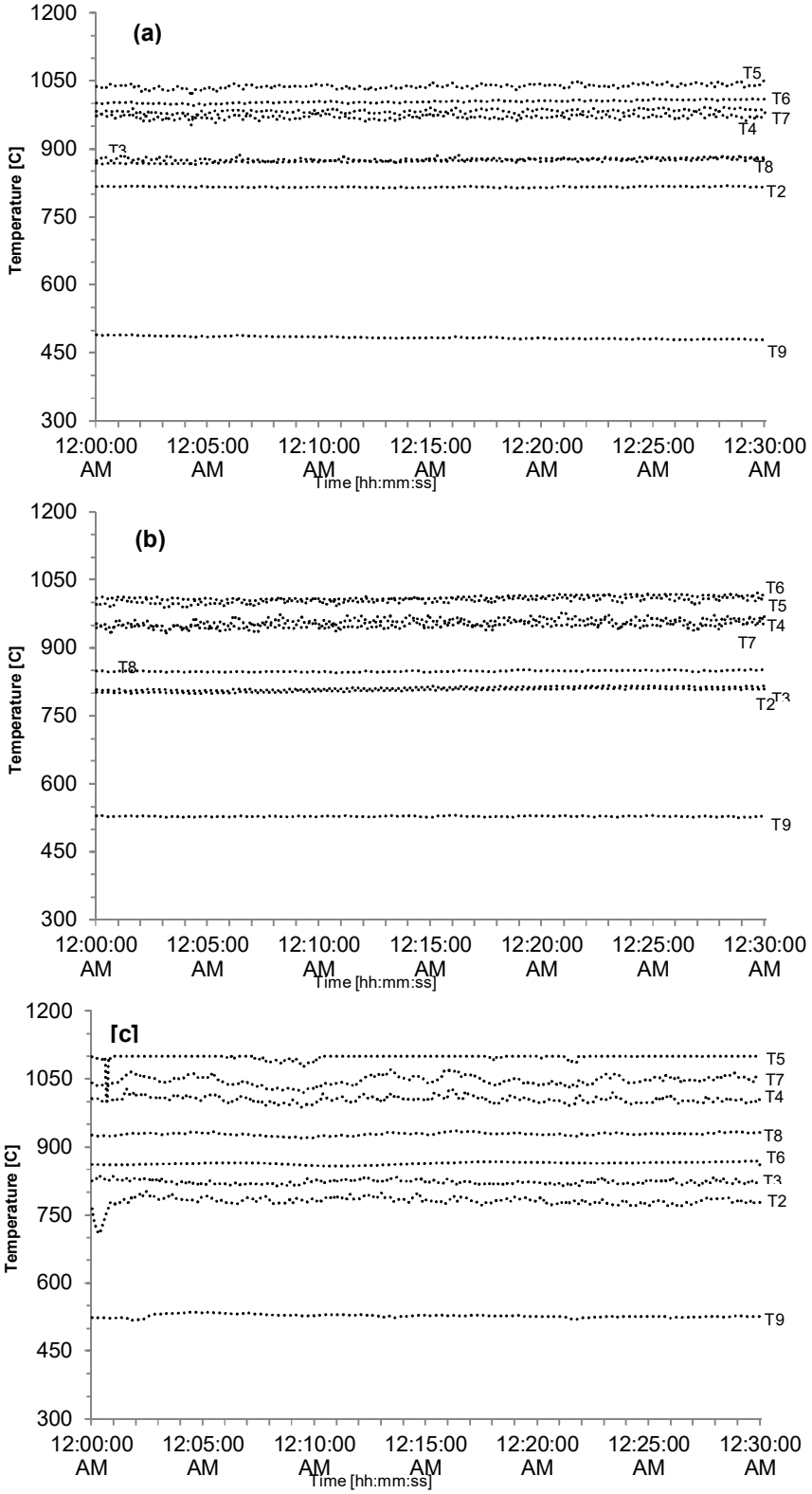

Figure 2. Vertical temperature profile along the BFB combustor operating at steady state condition during the combustion of chipped residual forest biomass derived from (a) – eucalypt; (b) – pine and (c) – golden wattle. T2 to T8 represent temperatures measured at thermocouples 2 to 8, at increasing height in the reactor. T9 is measured in the exhaust.

526

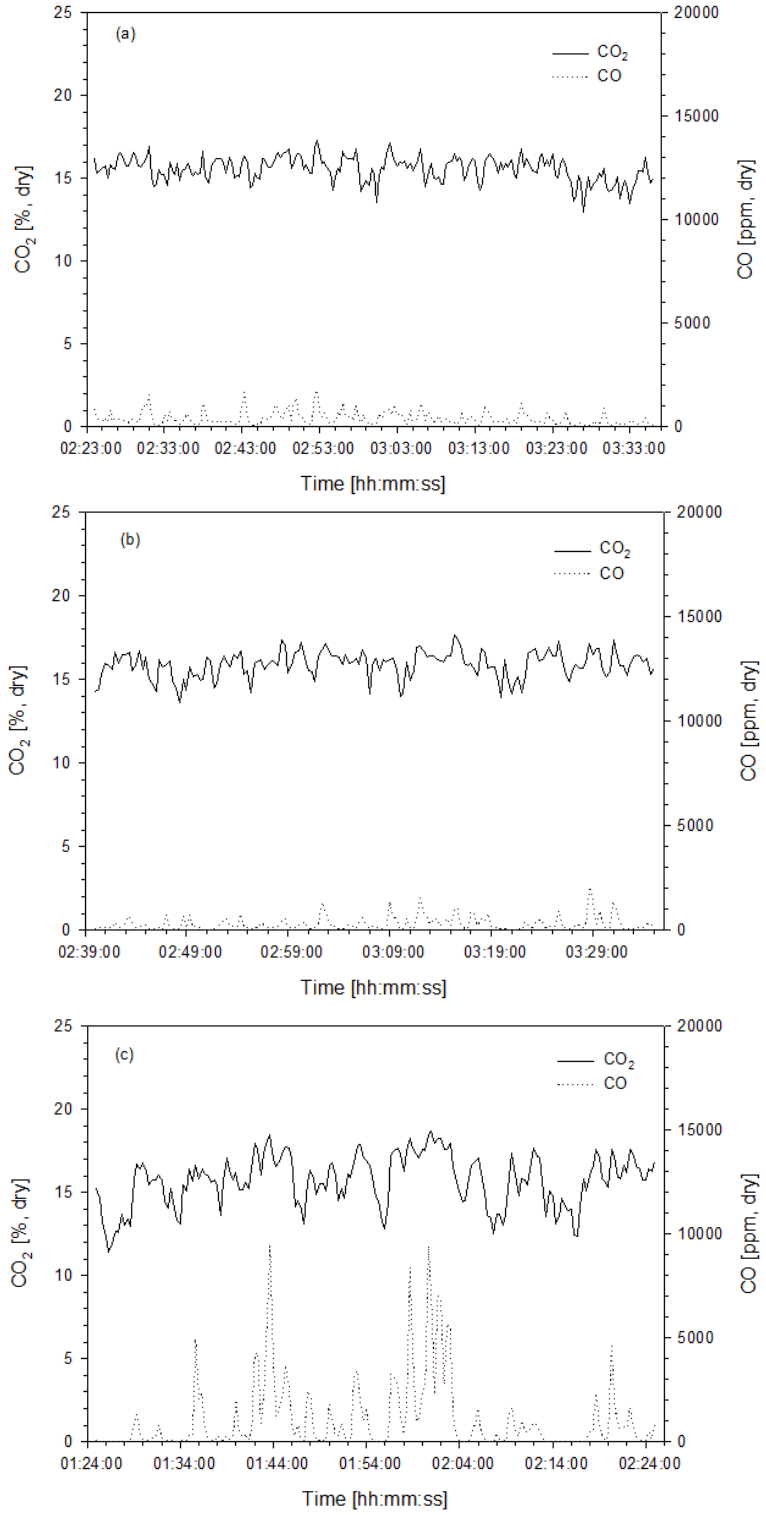

527 Figure 3. Composition of exit flue gas in terms of CO_2 (%, dry gas) and CO (ppm, dry gas) for combustion experiments
528 of (a) chipped eucalypt, (b) chipped pine and (c) chipped golden wattle

529

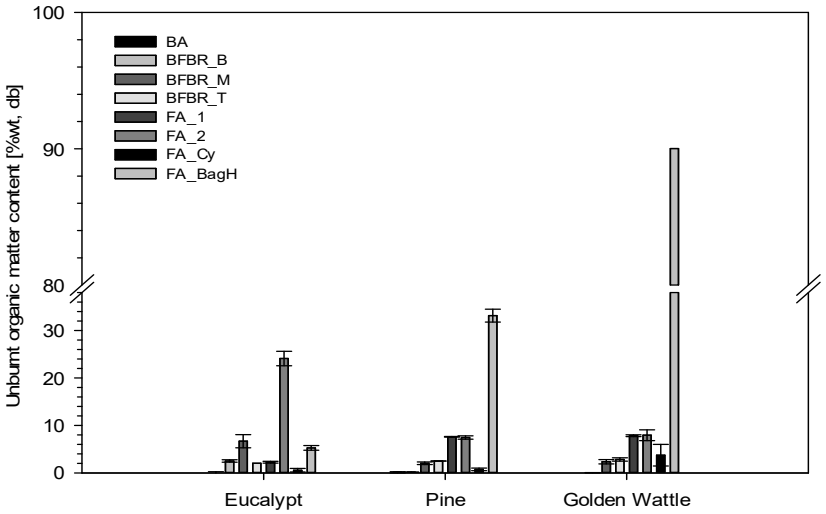

530

531 Figure 4. Unburnt organic matter content of the ashes collected at different points along the combustion system, for the
532 combustion experiments of eucalypt, pine and golden wattle (BA – bottom ash; BFBR_B/M/T – ashes collected from the
533 inside of the fluidised bed reactor, from the bottom/middle/top layers of height; FA_1/2 – ashes collected from the
534 exhaust duct 1st/2nd sections; FA_Cy – ashes collected from the cyclone separator; FA_BagH – ashes collected from
535 the baghouse filter)

536

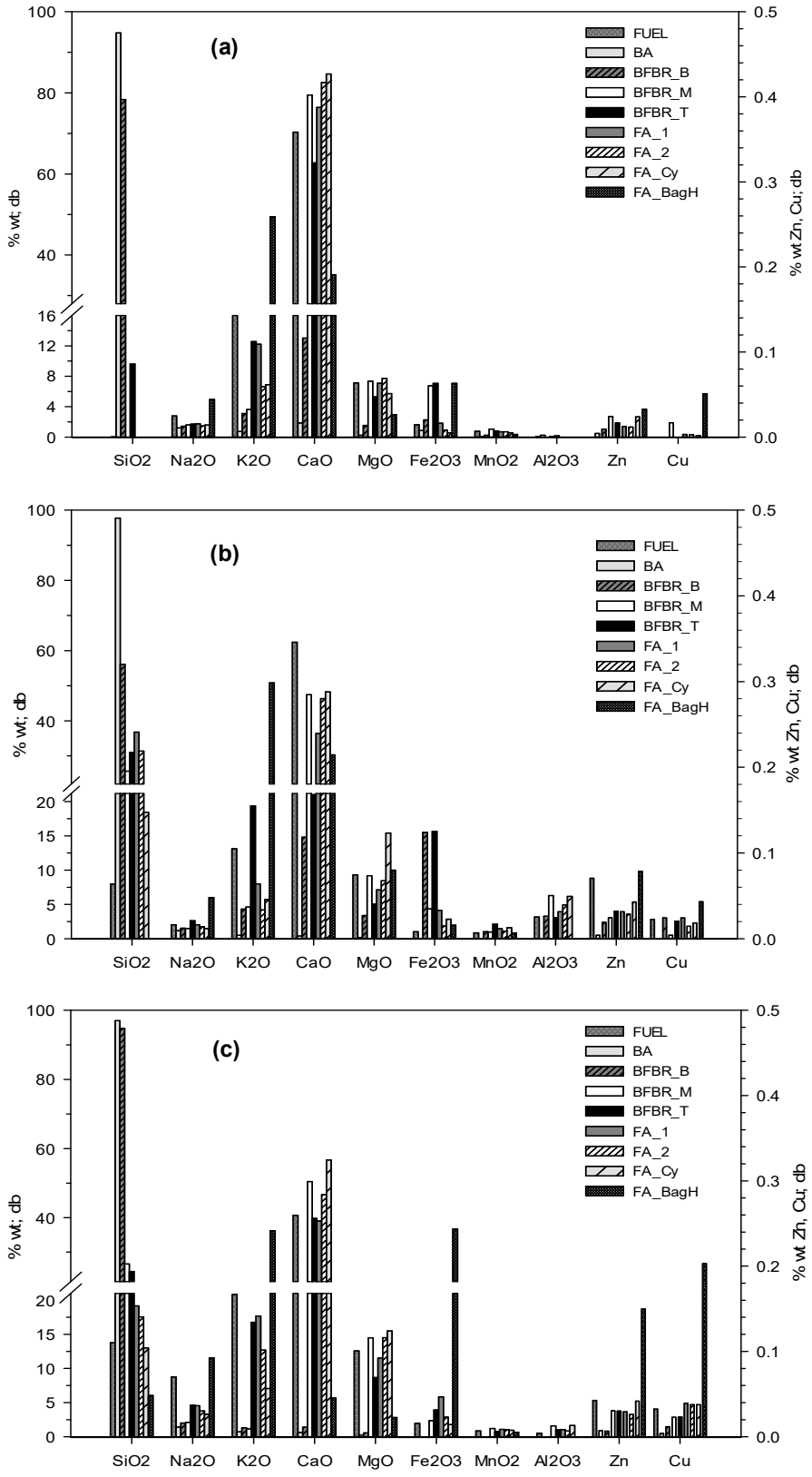

537

538 Figure 5. Chemical composition of the ashes expressed as oxides, for the combustion of (a) - chipped eucalypt; (b) –
539 chipped pine and (c) – chipped golden wattle. Values are normalized to the total mass fraction

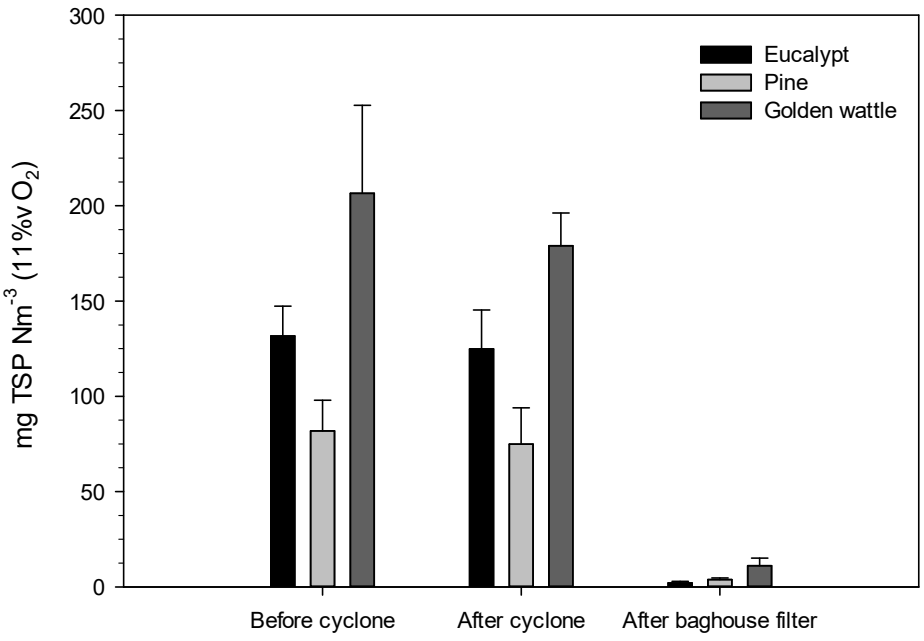

Figure 6. Particulate emissions (TSP concentrations normalised to 11%O_2), for the combustion of chipped eucalypt, pine and golden wattle